Biochar (2020) 2:121–134
https://doi.org/10.1007/s42773-020-00035-5

ORIGINAL ARTICLE

Biochars and their magnetic derivatives as enzyme-like catalysts mimicking peroxidases

Ivo Safarik[1,2] · Jitka Prochazkova[1] · Eva Baldikova[1] · Hans-Peter Schmidt[3] · Witold Kwapinski[4] · Ivo Medrik[2] · Petr Jakubec[2] · Mirka Safarikova[1] · Kristyna Pospiskova[2]

Received: 25 June 2019 / Accepted: 8 January 2020 / Published online: 10 February 2020

Abstract

Various materials have been extensively investigated to mimic the structures and functions of natural enzymes. We describe the discovery of a new catalytic property in the group of biochar-based carbonaceous materials, which are usually produced during biowaste thermal processing under specific conditions. The tested biochars exhibited peroxidase-like catalytic activity. Biomaterial feedstock, pyrolysis temperature, size of resulting biochar particles or biochar modification (e.g., magnetic particles deposition) influenced the peroxidase-like activity. Catalytic activity was measured with the chromogenic organic substrates *N*,*N*-diethyl-*p*-phenylenediamine (DPD) or 3,3′,5,5′-tetramethylbenzidine (TMB), in the presence of hydrogen peroxide. Magnetic biochar composite was studied as a complementary material, in which the presence of iron oxide particles enhances catalytic activity and enables smart magnetic separation of catalyst even from complex mixtures. The activity of the selected biochar had an optimum at pH 4 and temperature 32 °C; biochar catalyst can be reused ten times without the loss of activity. Using DPD as a substrate, K_m values for native wood chip biochar and its magnetic derivative were 220 ± 5 μmol L^{-1} and 690 ± 80 μmol L^{-1}, respectively, while V_{max} values were 10.1 ± 0.3 μmol L^{-1} min^{-1} and 16.1 ± 0.4 μmol L^{-1} min^{-1}, respectively. Biochar catalytic activity enabled the decolorization of crystal violet both in the model solution and the fish pond water containing suspended solids and dissolved organic matter. The observed biochar enzyme mimetic activity can thus find interesting applications in environmental technology for the degradation of selected xenobiotics. In general, this property predestines the low-cost biochar to be a perspective supplement or even substitution of common peroxidases in practical applications.

Keywords Peroxidase-like activity · Biochar · Magnetic iron oxides · Microwave synthesis

Electronic supplementary material The online version of this article (https://doi.org/10.1007/s42773-020-00035-5) contains supplementary material, which is available to authorized users.

✉ Ivo Safarik
ivosaf@yahoo.com

✉ Kristyna Pospiskova
kristyna.pospiskova@upol.cz

1 Department of Nanobiotechnology, Biology Centre, ISB, CAS, Na Sadkach 7, 370 05 Ceske Budejovice, Czech Republic

2 Regional Centre of Advanced Technologies and Materials, Palacky University, Slechtitelu 27, 783 71 Olomouc, Czech Republic

3 Ithaka Institute for Carbon Strategies, Ancienne Eglise 9, Arbaz, Switzerland

4 Chemical Sciences Department, Bernal Institute, Faculty of Science and Engineering, University of Limerick, Limerick, Ireland

Abbreviations

A_{551}	Absorbance values at wavelength 551 nm
AA	Ascorbic acid
BCH	Biochar
(M)BC1-3, LIM1-3, OL1-8, MC, IND	various types of biochars (detailed info. in Table 1)
C	Catalyst (BCH or IOP)
COD	Chemical oxygen demand
CNTs	Carbon nanotubes (SW—single walled)
CS	Chromogenic substrate (DPD or TMB)
CV	Crystal violet
CVM	Cyclic voltammetry measurement

Table 1 Overview of biochar samples used for experiments

Designation	Feedstock	Max. temp. [°C]	Time at max. temp. [min]	Atmosphere	Instrumentation	Provided by	Characterization
BC1	Shavings from wood chip production	620	20	No inert gas used	PYREG 500—III pyrolysis units (PYREG GmbH, Dörth, Germany)	Swiss Biochar (Lausanne, Switzerland)	Bachmann et al. (2016)
BC2	Blend of paper sludge and wheat husks	500	20	No inert gas used		Sonnenerde GmbH (Riedlingsdorf, Austria)	Bachmann et al. (2016)
BC3	Sewage sludge	600	20	No inert gas used		PYREG GmbH (Dörth, Germany)	Bachmann et al. (2016)
LIM1	*Miscanthus* × *giganteus*	300	60	No inert gas used	Temperature controller cabinet, a quartz tube reactor, and an electric furnace heater (Limerick, Ireland)	WK	Trazzi et al. (2016)
LIM2	*Miscanthus* × *giganteus*	500	60	No inert gas used		WK	Trazzi et al. (2016)
LIM3	*Miscanthus* × *giganteus*	700	60	No inert gas used		WK	Trazzi et al. (2016)
OL1	Sawdust (hard wood—oak)	700	240	Nitrogen	Material was heated in a porcelain dish from room temperature (temperature gradient 7 °C/min) to 600 or 700 °C for 1 or 4 h in tube laboratory furnace (LAC, s.r.o., Rajhrad, Czech Republic)	IM	–
OL2	Sawdust (soft wood—spruce, pine)	700	240	Nitrogen		IM	–
OL3	Sawdust (soft wood—spruce)	600	60	Nitrogen		IM	–
OL4	Sawdust (soft wood—spruce)	700	240	Nitrogen		IM	–
OL5	Spent coffee grounds	600	240	Nitrogen		IM	–
OL6	Spent coffee grounds	700	240	Nitrogen		IM	–
OL7	Orange peel powder	700	240	Nitrogen		IM	–
OL8	Cellulose powder	700	240	Nitrogen		IM	–
MC	Maize cob biochar produced by a small local producer						
IND	Biochar obtained from the industrial wood gasification plant						

WK Witold Kwapinski *IM* Ivo Medrik

DPD	*N,N*-diethyl-*p*-phenylenediamine
GCE	Glassy carbon electrode
GO	Graphene oxide (r—reduced)
GQDs	Graphene quantum dots
HRP	Horseradish peroxidase
IOP	Magnetic iron oxide particles prepared by microwave-assisted synthesis
K_m	Michaelis constant
NPs	Nanoparticles
NRs	Nanorods
TMB	3,3′,5,5′-tetramethylbenzidine
V_{max}	Maximal reaction velocity
WK, IM	biochar suppliers (detailed info. in Table 1)

1 Introduction

The current trend of chemical and biotechnology industries is the supports greener, environmentally-friendlier and more sustainable catalytic processes. Catalysts may be classified as either homogeneous or heterogeneous. Homogeneous catalysis uses soluble catalysts in the same phase with reactants, while heterogeneous catalysis occurs at the interface of two phases with the catalyst in a different phase from the reactants. Possible bridges between these approaches ("semi-heterogeneous" catalysis, with nanoparticles as an example), have been discussed (Astruc et al. 2005). An important step during heterogeneous catalytic processes is the possibility of an easy catalyst recycling after the reaction and its reusability in the next cycle. This is a substantial benefit. Heterogeneous catalysts have, therefore, obvious advantages in regard to environmental impacts and sustainable developments. Bio-based catalysis employing variety of enzymes is of special interest; solid-phase biocatalysts can be economically tailored on large scale applications in various areas of biotechnology, food technology and environmental technology (Bilal et al. 2017; Chuah et al. 2017; Varma 2016).

Various compounds including biomolecules, dendrimers, polymers, porphyrins, metal complexes or cyclodextrins have been studied to imitate the functions and structures of natural enzymes (Wei and Wang 2013). Compared to natural enzymes, enzyme-like systems (also known as pseudo-enzymes or artificial enzymes) may provide enormous advantages in terms of easy preparation, low cost, better thermal stability, pH tolerance and long-term storage.

Discovery of the peroxidase-mimetic activity of ferromagnetic nanoparticles in 2007 (Gao et al. 2007) inspired the investigation of other potential peroxidase-like systems based on metallic and carbonaceous (nano)materials or their mixtures. Gold nanoparticles (Deng et al. 2016), ceria nanorods (Tian et al. 2015), cupric oxide nanoparticles (Chen et al. 2012), Cu^{2+} ions (Zheng et al. 2016), diverse bimetallic nanoparticles (Jiang et al. 2016; Zhang et al. 2015), $FeVO_4$ nanobelts (Yu et al. 2016), iron phosphate microflowers (Wang et al. 2012b) and many other nanomaterials have been successfully used to catalyze peroxidase substrates oxidation in the presence of H_2O_2 (Wei and Wang 2013).

The level of peroxidase-like activity can be significantly altered with appropriate modification or functionalization. It was observed that Fe_3O_4–Au nanoparticles exhibited better catalytic properties than the pure Fe_3O_4 aggregates (Sun et al. 2013), while unmodified Au nanoparticles had higher activity than the amino-modified or citrate-capped ones (Wang et al. 2012a).

In addition, size and shape of nanoparticles considerably influence the enzyme-like activity, as shown in the catalytic activity of Fe_3O_4 nanoparticles which increased with the reduction of nanoparticle size (Peng et al. 2008). However, when the size and shape dependence of $MnFe_2O_4$ particles were studied, the peroxidase-like activity was as follows: 4 nm (spherical) > 18 nm (plate-like) > 27 nm (near cubic) > 16 nm (spherical) (Peng et al. 2015). Shape studies were also carried out on $CoFe_2O_4$ particles, where the level of peroxidase-like activity in the order of spherical > near corner-grown cubic > starlike > near cubic > polyhedron was observed; this order was closely related to their particle size and crystal morphology (Zhang et al. 2015). Also the shape of Fe_3O_4 nanoparticles influenced their peroxidase-mimetic properties, following the order sphere > cube > octahedron > hexagonal plate, which was related to the surface Fe(II)/Fe(III) ratios or crystal planes (Wan et al. 2016).

Magnetic nanoparticles of magnetite or maghemite, as an inner part of a spherical biomacromolecule magnetoferritin surrounded by a protein shell, also exhibited peroxidase-like activity, which increased with increasing loading factor determining the iron content (Melnikova et al. 2014).

Peroxidase-like systems can be utilized in diverse areas of bioscience, medicine and environmental technology. New types of peroxidase-mimetic (nano)particles have been successfully employed as a component of biosensors for the detection of cancer (Tian et al. 2015; Zheng et al. 2016), glucose (Ding et al. 2016), H_2O_2 (Qiao et al. 2014), heavy metal ions (Chen et al. 2015), cholesterol (Hayat et al. 2015) and pathogenic bacteria (Jiang et al. 2016; Park et al. 2015), as well as, for degradation of xenobiotics (Guo et al. 2015; Mu et al. 2016; Wan et al. 2016), or for inhibition of bacterial growth and biofilm elimination (Gao et al. 2014).

Also carbon-based materials, including graphene-based nanomaterials (Garg et al. 2015), graphene quantum dots (Sun et al. 2015), helical carbon nanotubes (Cui et al. 2011), carbon nanotubes with self-assembled hemin (Zhang et al.

2013), carbon nanodots (Safavi et al. 2012; Zhu et al. 2014), carboxyfullerenes (Li et al. 2013a) or hydrophilic mesoporous carbon (Huang et al. 2013) often exhibit peroxidase-like activity.

Exceptional interest in nanozymes resulted in several extended review papers covering in detail their classification, catalytic mechanisms, activity regulation and applications in biosensing, environmental protection, disease treatments and other applications (Golchin et al. 2017; Huang et al. 2019; Wu et al. 2019).

Recently, biochar produced by pyrolysis of agricultural waste has become an intensively studied carbon-based material. Biochar production represents a typical example of a circular bio-economy process. The produced biochar is mainly used in agriculture as an efficient soil amendment (El-Naggar et al. 2019a, b) or as an adsorbent for waste water treatment (Oliveira et al. 2017; Qambrani et al. 2017). However, biochar can be also used as a catalyst or microbial fuel cell electrode (Lee et al. 2017). Cu(II)-polluted biomass was converted into an environmentally benign Cu nanoparticle-embedded biochar composite exhibiting cyanobacteria inhibition (Li et al. 2019).

Based on the previous research results associated with the peroxidase-like activity of carbon-based materials, this study was targeted to investigate possible peroxidase-mimetic activity also in the group of biochar-based materials originating from pyrolysis of plant biomass. No similar study dealing with peroxidase-like activity of biochar-based materials has been published yet. Different levels of peroxidase-mimetic activity were obtained for biochars produced from various biomass feedstock under different pyrolysis conditions. Furthermore, the influence of subsequent magnetic modification of biochars with microwave-synthesized magnetic iron oxide nano- and microparticles (Safarik et al. 2016; Safarik and Safarikova 2014) was tested. This modification led to magnetically responsive composites with deposited magnetic particles and their aggregates on the surface of native biochar, exhibiting increased peroxidase-like activity. Basic characterization of biochar peroxidase-like activity is described in this paper, based on the testing of various types of biochars and their catalytic reaction towards chromogenic organic substrates specific for peroxidase enzymes. A practical application of biochar-based materials in environmental technologies was demonstrated by the catalytic organic dye decolorization.

2 Materials and methods

2.1 Materials

Biomass feedstocks used for the biochar production, the biochar production technology (pyrolytic units), and pyrolysis reaction conditions (temperature and duration of pyrolytic process, special atmosphere) are presented in Table 1. Extensive characterization of the biochars BC1–BC3 and LIM1–LIM3 has been published (Bachmann et al. 2016; Trazzi et al. 2016). Several biochar samples were prepared under laboratory conditions in a furnace (samples OL1–8). In addition, two industrial biochar samples were used during our experiments (samples MC and IND). Individual biochars were ground if necessary and sieved to obtain a fraction between 100 and 250 µm. Selected biochar samples were magnetically modified using microwave-synthesized magnetite as described previously (Safarik et al. 2016; Safarik and Safarikova 2014). α-Cellulose powder, *N,N*-diethyl-*p*-phenylenediamine sulfate salt (DPD), crystal violet (CV; C.I. 42555), 30% (w/w) hydrogen peroxide solution and disodium hydrogen phosphate were obtained from Sigma-Aldrich, Czech Republic. TMB substrate solution (TMBL01, containing hydrogen peroxide, chromogene 3,3′,5,5′-tetramethylbenzidine and stabilizing agents) was supplied by Enzymo Plus, Czech Republic. Common chemicals (e.g., ferrous sulfate heptahydrate, sodium hydroxide, ascorbic acid (AA), sodium citrate monohydrate, etc.) were obtained from Lach-Ner and crystal violet from Lachema, Czech Republic. All chemicals were analytical reagents grade and were used without further purification. All stock solutions for electrochemical measurements were prepared with deionized water (18 MΩ cm^{-1}). Water samples from three typical fish farming ponds in South Bohemian and South Moravian regions (Zdrahanka pond, 48.9990175 N, 14.3983494 E, pH 7.3, COD_{Cr} 52.5 mg L^{-1}; Klimsak pond, 49.4085415 N, 16.6343234 E, pH 8.1, COD_{Cr} 43.8 mg L^{-1}; Karolin pond, 49.4076739 N, 16.6614586 E, pH 8.0, COD_{Cr} 50.2 mg L^{-1}) were used to study crystal violet decolorization.

2.2 Determination of peroxidase-like activity

Ten milligram of sample (various types of biochar) was mixed with 3400 µL of distilled water and preincubated for 2 min. Then, 400 µL of DPD substrate (12.5 mM stock solution in water) and 200 µL of hydrogen peroxide substrate [2% (v/v) stock solution in water] were added. Reaction mixture was shortly mixed on a vortex and incubated at 22 °C for 4.5 min on an automatic rotator (20 rpm). The reaction mixture was then immediately filtered through a filter paper and the filtrate was collected from the first 30 s of filtration. Finally, the absorbance of the filtrate, containing a purple-colored reaction product, was measured spectrophotometrically at 551 nm. Using a TMB substrate, 10 mg of preincubated sample in 2000 µL water was mixed with 2000 µL of a commercial TMB solution and incubated for 4.5 min on the rotator, then separated by centrifugation. Increasing absorbance of the blue–green colored product was monitored

spectrophotometrically at 655 nm. In both cases, corresponding blanks (the same reaction mixture and conditions but without biochar) were subtracted from measured absorbance values. Peroxidase-like activity was expressed as an absorbance of the reaction mixture at 551 nm using DPD substrate. Measurements were performed at least in triplicate.

To study the effect of pH on the peroxidase-like activity of biochars, Britton–Robinson buffer, pH 2–12, was used instead of water.

To study the operational stability of biochar catalyst, the reaction was repeated ten times with the same sample (washing of sample with water after each cycle; short centrifugation used for biochar separation).

The study of peroxidase-like kinetics was performed using Michaelis–Menten model, DPD concentration was in range 313–5000 μmol L^{-1}, with constant hydrogen peroxide concentration [0.5% (v/v) in reaction solution].

To verify the role of the reactive oxygen species in the peroxidase-like reaction, ascorbic acid was added into the standard reaction mixture (in concentration range from 0.15 to 1.5 mmol L^{-1}).

2.3 Decolorization of organic dye

Ten milligrams of biochar sample was mixed with 5 mL of organic dye water solution (crystal violet, 50 μg mL^{-1}), followed immediately by the addition of hydrogen peroxide [to final concentration 1% (v/v) in solution]. Reaction mixture was mixed on automatic rotator for appropriate time (e.g., 5–20 min). Then, 1 mL of reaction mixture was collected and centrifuged. Decrease of the crystal violet dye concentration was observed spectrophotometrically, measuring the absorption spectrum of the residual dye in the supernatant (maximum at 591 nm). Also control sample with added water instead of hydrogen peroxide was tested for comparison, as well as the crystal violet dye solution with added hydrogen peroxide (without biochar sample). To verify the role of the reactive oxygen species in the decolorization reaction, ascorbic acid was added into the standard reaction mixture (1.12 mmol L^{-1}).

2.4 Electrochemical measurements

Cyclic voltammetry measurements (CVMs) were performed using a Metrohm Autolab PGSTAT128N instrument (Metrohm Autolab B.V., The Netherlands). Obtained data were evaluated with incorporated NOVA software package (version 1.11.2). The three-electrode setup [working electrode: glassy carbon electrode (GCE, 3 mm in diameter, 2Theta Company: Czech Republic); auxiliary electrode: platinum wire; reference electrode: Ag/AgCl (3 mol L^{-1} KCl)] was employed as a suitable candidate for electrochemical characterization of biochar sample. Citrate–phosphate buffer ($c = 0.2$ mol L^{-1}; pH 3.8) was used as a supporting electrolyte for all measurements. All experiments were carried out at room temperature (22 ± 2 °C). Glassy carbon electrodes were first polished on wet silicon carbide paper using 1 and 0.05 μm Al_2O_3 powder sequentially and then washed in water and ethanol, respectively. Modification of GCE working electrode was performed by drop-coating technique: 10 μL drop of biochar suspension (5 g L^{-1}) was coated onto the GCE surface and allowed to dry at ambient temperature to form a thin film.

3 Results and discussion

3.1 Determination of peroxidase-like activity

To detect the peroxidase-like activity of 16 types of biochar (see Table 1), two typical peroxidase chromogenic co-substrates were tested, namely, *N,N*-diethyl-*p*-phenylenediamine (DPD) and 3,3′,5,5′-tetramethylbenzidine (TMB). Hydrogen peroxide—based oxidation of DPD leads to the formation of the radical cation DPD^+, which produces a stable purple color with absorption at 551 nm. The H_2O_2 oxidation of TMB leads to the formation of a blue reaction product with absorption at 655 nm. All biochar types tested caused color

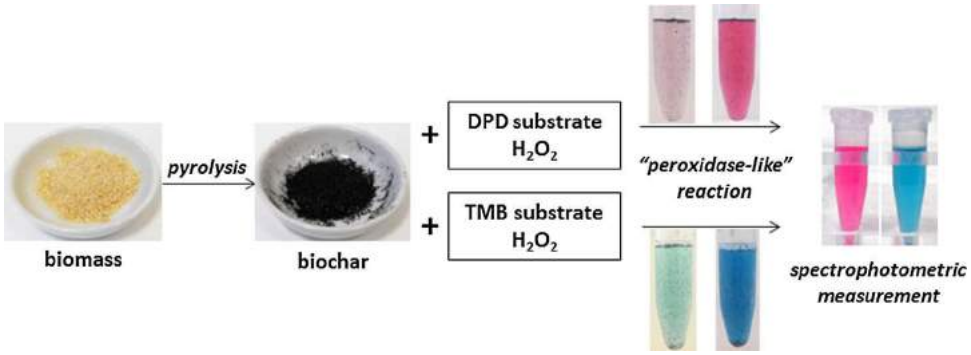

Fig. 1 Scheme of biochar preparation and its peroxidase-like activity determination using DPD and TMB co-substrates in the presence of hydrogen peroxide, followed by spectrophotometric measurement of the colored reaction product (color online)

change of both peroxidase co-substrates (see Fig. 1). For subsequent experiments only DPD co-substrate was used.

To evaluate the results of peroxidase-like activity of biochars, measured absorbance values of the colored reaction products were used. However, units typical for standard expression of enzyme activity are not accurate for biochar studies due to their adsorption properties, thus partially decreasing the amount of free reaction products available for photometric measurements. Adsorption properties of biochar will be discussed in the following part. Therefore, only arbitrary values of specific enzyme-like activity of biochar samples are mentioned as the values expressing the overall enzyme-like activity not taking into account the possible adsorption of the reaction product.

Table 2 shows average values of peroxidase-like activity (using DPD co-substrate, expressed as absorbances at 551 nm) of the tested biochar samples and calculated theoretical values of specific enzyme-like activity of biochars (expressed in nkat per mg of biochar). In some cases, great variability of absorbances was observed in repeated measurements of single biochar samples which may be explained by biochar microheterogeneity. In general, biochar-based materials are not considered as homogeneous and unique materials (EBC 2019). General biochar types are based on the feedstock used, pyrolysis conditions and post-pyrolysis treatment, which leads to microheterogeneity due to natural variations within the biomass feedstock (e.g., mineral content and organic constitution) as well as heat and gas transfer variations within pyrolyzed particles. For this reason, rather high standard deviations are observed. However, variations in peroxidase-like activities of different biochars due to different feedstock and pyrolysis parameters predominated.

In principle, different types of biochar with peroxidase-mimicking activities can be roughly classified into two types. For the first type, the peroxidase-like activities are solely based on the carbon structure of biochars. For the second type, the activities are derived from the catalytic materials assembled into biochar (especially metal ions). Based on the fact that biochar prepared from chemically pure cellulose exhibited peroxidase-like activity, it can be concluded that the peroxidase-mimicking activity is primarily caused by biochar itself, and not due to the presence of accompanying metal residues. However, potential effect of metal ions naturally present in biochars of plant origin (Bachmann et al. 2016) cannot be excluded for specific biochar types (e.g., biochars prepared from plants growing at localities with high concentration of heavy metal ions).

Due to the fact that biochar-based materials exhibit adsorption properties (Safarik et al. 2016; Sewu et al. 2017), possible adsorption of the colored reaction product on biochars need to be also considered. To test the ability of biochars to adsorb the oxidized co-substrate DPD, samples with lower peroxidase-like activity were tested by incubation with the purple-colored reaction product formed by sample OL6. Each of the tested biochar samples (OL1–5 and OL7–8) exhibited adsorption of the oxidized co-substrate in the range between 18% and 52% (see Table 3) using the following reaction conditions: 10 mg of biochar, 4 mL of oxidized DPD ($A_{551} = 0.79$), 4.5 min incubation at 22 °C, 30 s filtration, 3 measurements. Thus, it has to be taken into account that the low measured peroxidase-like activity of various biochar samples can also be caused by their adsorption properties. Nevertheless, the activity of all tested biochar-based materials was clearly confirmed by the described

Table 3 Adsorption of oxidized co-substrate DPD on selected types of biochar samples

Sample	Adsorbed amount of oxidized DPD on biochar (%)
OL1	30 ± 1
OL2	26 ± 1
OL3	28 ± 4
OL4	19 ± 2
OL5	42 ± 2
OL7	52 ± 5
OL8	18 ± 2

Table 2 Average values of peroxidase-like activity (expressed as A_{551}, using DPD as co-substrate) and arbitrary values of specific activity of the tested biochar samples

Sample	A_{551}	Arbitrary specific enzyme-like activity (nkat mg^{-1})	Sample	A_{551}	Arbitrary specific enzyme-like activity (nkat mg^{-1})
BC1	0.639 ± 0.139	0.0406	OL1	0.080 ± 0.004	0.0051
BC2	0.502 ± 0.051	0.0319	OL2	0.230 ± 0.024	0.0146
BC3	0.953 ± 0.106	0.0605	OL3	0.155 ± 0.001	0.0098
LIM1	0.121 ± 0.014	0.0077	OL4	0.100 ± 0.009	0.0063
LIM2	0.296 ± 0.044	0.0188	OL5	0.055 ± 0.007	0.0035
LIM3	0.605 ± 0.032	0.0384	OL6	0.790 ± 0.087	0.0502
IND	0.584 ± 0.067	0.0371	OL7	0.125 ± 0.005	0.0079
MC	0.253 ± 0.013	0.0161	OL8	0.158 ± 0.013	0.0100

activity measurements. As already mentioned, the arbitrary enzyme-like activity values were not corrected considering these adsorption effects because the reaction product adsorption is highly individual for any biochar type.

The study of peroxidase-like kinetics is fundamental and necessary to understand the enzyme-like characteristics of biochars, and the enzyme kinetic constant K_m (Michaelis constant) and V_{max} (maximal reaction velocity) are one of the most important factors for the evaluation of the enzyme and enzyme-like materials efficiency (lower K_m values are connected with higher affinity to substrate). The peroxidase-like behavior of the typical biochar (BC1, prepared from wood chips) and its magnetically modified form (MBC1; see Chapter 3.5) was examined at room temperature using DPD as a chromogenic substrate. Absorbance data were converted to concentration by the Beer–Lambert Law using a molar absorption coefficient of 21,000 M^{-1} cm^{-1} for DPD-derived oxidation product (Bader et al. 1988). Figure S1 demonstrates typical Michaelis–Menten curves (after fitting) for peroxidase-like catalytic reaction of samples BC1 and MBC1. The obtained values of K_m for chromogenic substrate DPD (native biochar BC1: $K_m = 220 \pm 5$ µmol L^{-1}, $V_{max} = 10.1 \pm 0.3$ µmol L^{-1} min^{-1}; magnetically modified biochar MBC1: $K_m = 690 \pm 80$ µmol L^{-1}, $V_{max} = 16.1 \pm 0.4$ µmol L^{-1} min^{-1}) were compared with analogous data for horseradish peroxidase (HRP, a typical peroxidase enzyme from oxidoreductases class, EC 1.11.1.7, widely used in various biochemical and biotechnology applications) and selected peroxidase-like materials (see Table 4). The obtained values are comparable with results from selected published studies. Examples demonstrate the dependence of K_m on the type of material, particle shape and size, and also on the decoration of target materials by other particles.

Various types of carbon nanomaterials exhibit intrinsic peroxidase-like activity. Mechanisms of the catalytic reactions have not been sufficiently clarified. One of the possible mechanisms has been described by Sun et al. (2015). During their studies with graphene quantum dots (GQDs), they have observed their high enzyme-like activity. The studied GQDs were mainly covered with carboxylic, carbonyl and hydroxy groups on their surface. After selective deactivation of these oxygen groups by specific titrants, they identified their different functions; the –C=O groups are present in catalytically active sites, the O=C–O– groups are part of substrate-binding sites and –C–OH groups can be involved in the inhibition of the catalytic activity (Sun et al. 2015). Based on the fact that biochar can contain similar oxygen containing groups, the enzyme-like mechanism both in biochars and GQDs can be similar. Another study focuses on the role of persistent free radicals in H_2O_2 activation by biochar, which can be implied in the degradation of organic contaminants. Fang et al. investigated that hydrogen peroxide can be activated by biochar, which is connected with the production of hydroxyl radicals to degrade 2-chlorobiphenyl. Persistent radicals present in biochar are the main contributor to the formation of hydroxyl radicals (Fang et al. 2014). Recent advances in biochar-based catalysis, applicable for pollution remediation, are summarized in a review (Wang et al. 2019).

Table 4 Values of Michaelis constant (K_m) for selected peroxidase-like materials and horseradish peroxidase

Catalyst	Chromogenic substrate (CS)	K_m [mmol L^{-1}] for CS	References
Enzymes			
HRP	DPD	0.696	Chang et al. (2009)
HRP	TMB	0.434	Gao et al. (2007)
HRP	TMB	0.415	Tian et al. (2015)
HRP	TMB	0.501	Li et al. (2013a)
HRP	TMB	0.400	Peng et al. (2008)
HRP	TMB	0.400	Cui et al. (2011)
HRP	TMB	0.275	Song et al. (2010)
HRP	TMB	0.580	Wu et al. (2014)
Metal oxide/metal nanoparticles			
Fe_3O_4 NPs	TMB	0.098	Gao et al. (2007)
Fe_3O_4 aggregates	TMB	0.179	Sun et al. (2013)
Fe_3O_4 NPs	TMB	0.270	Peng et al. (2008)
Fe_3O_4 NPs	DPD	0.627	Chang et al. (2009)
Fe_3O_4–Au	TMB	0.011	Sun et al. (2013)
$MnFe_2O_4$ NPs	TMB	0.112	Peng et al. (2015)
Spherical (4 nm)		0.242	
Plate-like (18 nm)		0.304	
Spherical (27 nm)		0.543	
Spherical (16 nm)			
$FeVO_4$	TMB	0.691	Yu et al. (2016)
NRs of ceria (porous)	TMB	0.147	Tian et al. (2015)
Carbon-based materials and derivatives			
C_{60}-carboxyfullerene	TMB	0.233	Li et al. (2013a)
Helical CNTs	TMB	0.020	Cui et al. (2011)
Au NPs-SW CNTs	TMB	0.480	Haider et al. (2015)
ZnO NPs-CNTs	ABTS	0.500	Hayat et al. (2015)
GQDs	ABTS	10.4	Sun et al. (2015)
GQDs-Fe_3O_4	TMB	0.050	Wu et al. (2014)
GO-Fe_3O_4	TMB	0.080	Wu et al. (2014)
GO-COOH	TMB	0.024	Song et al. (2010)
rGO	TMB	0.340	Xie et al. (2013)
rGO-Co_3O_4	TMB	0.190	Xie et al. (2013)
Biochar BC1	DPD	0.220	This paper
Biochar MBC1	DPD	0.690	This paper

To verify the possible role of reactive oxygen species associated with the peroxidase-like reaction of biochar, experiments using ascorbic acid (AA) added to the reaction mixture (as a scavenger of hydroxyl and superoxide radicals) have been performed (Dong et al. 2018). In our study, we have also tested possible quenching of these radicals by ascorbic acid. Catalytic activity of biochars was affected (inhibited) by the presence of AA in a different way, according to the type of biochar (the reaction was inhibited at different intensities, in connection with the amount of radicals formed). The effect of various concentration of ascorbic acid on peroxidase-like reaction was demonstrated on BC1 sample (Fig. S2). Based on this fact, the generation of radicals also plays an important role in the catalytic mechanism. We have further performed electrochemical measurements (cyclic voltammetry) to get more information about redox processes and radicals after interaction of biochar with hydrogen peroxide in buffer solution, results will be discussed in the Subchapter 3.6.

For each solid catalyst, reusability is an important property for practical utilization from an economical point of view. Using MC biochar, reaction with DPD substrate was repeated ten times without the loss of catalytic activity.

3.2 Effect of pyrolysis conditions on peroxidase-like activity of biochar

An interesting dependence was observed for *Miscanthus* × *giganteus* biochar prepared at different temperatures at constant pyrolysis time (LIM1–3). Increase of pyrolysis temperature led to the significant increase in peroxidase-like activity (see Fig. 2a). A similar effect was also detected for the biochars prepared from spent coffee grounds, where the measured activity of the sample pyrolyzed at 700 °C was approximately 14-times higher than the activity of the sample prepared at 600 °C.

In the case of *Miscanthus* biochar the increase of pyrolysis temperature led to the increase of both the carbon contents (63.6%; 86.3% and 90.4%) and BET surface area (6.39; 81.0 and 244 $m^2\ g^{-1}$) for the temperatures 300 °C, 500 °C and 700 °C and pyrolysis time 60 min (Trazzi et al. 2016). The selected atomic ratios (i.e., H/C and O/C) sharply decreased, suggesting that with increasing charring temperature, the relative degree of aromaticity (H/C ratio) and polarity (O/C ratio) markedly decreased, which could be attributable to the development of functional groups (Li et al. 2013b; Trazzi et al. 2016). It has been also observed by other authors that heteroaromatic *N*-structures are formed during the pyrolysis process; it is expected that *N*-bound in heterocyclic compounds is chemically stable (Singh et al. 2014).

A detailed study of rice straw and rice bran biochar pyrolyzed at different temperatures using solid-state ^{13}C NMR spectroscopy has been performed recently (Li et al. 2013b). Development of functional groups during the charring process was observed; their development rate followed the following order: fused-ring aromatic structures > aromatic C–O groups > aliphatic *O*-alkylated (HCOH) carbons ≈ anomeric O–C–O carbons (Li et al. 2013b). Increased number of oxygen containing groups in the biochar pyrolyzed at increased

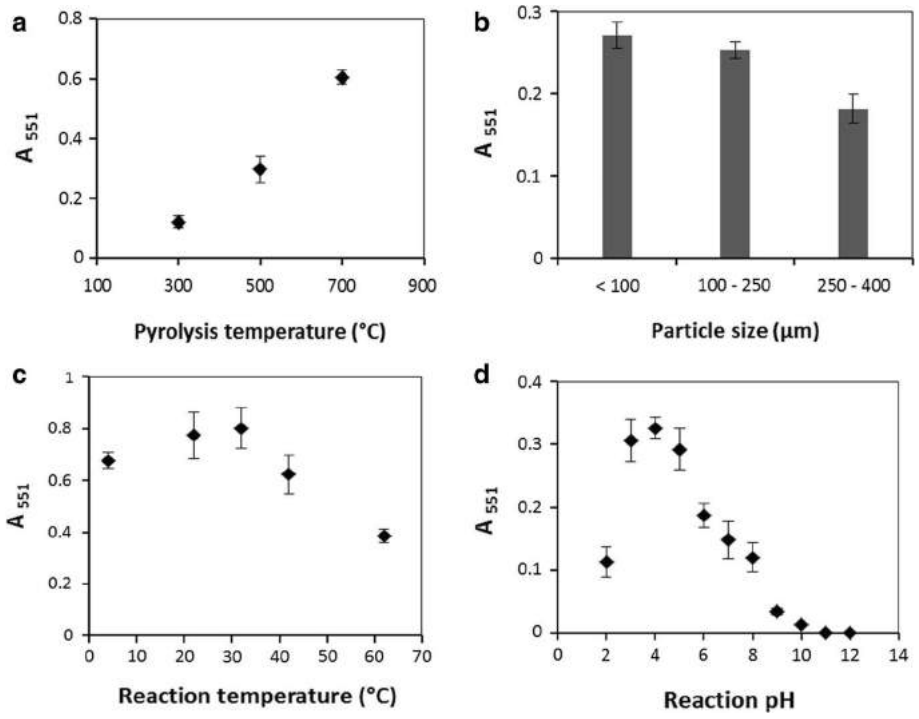

Fig. 2 **a** Dependence of peroxidase-like activity of *Miscanthus x giganteus* biochar (LIM1-3) on the temperature of the pyrolysis treatment at constant pyrolysis time. **b** Dependence of peroxidase-like activity of maize cob biochar (MC) on the size of its particles. **c** Dependence of peroxidase-like activity of wood chip biochar BC1 on the reaction temperature. **d** Dependence of peroxidase-like activity of the wood chip biochar BC1 on the pH value of the reaction mixture

temperature together with the increased surface area, could explain the higher enzyme-like activity observed in *Miscanthus × giganteus* biochar pyrolyzed at higher temperature. It has to be noticed, however, that biochar pyrolyzed at very high temperatures did not contain measurable amounts of oxygen containing groups, but its peroxidase-like activity was very high (sample IND; its FTIR measurement has not detected any peak corresponding to oxygen containing groups similarly to other biochars prepared at high temperatures (Asada et al. 2004). Most probable alternative mechanism has to be suggested for carbon rich, oxygen depleted biochars.

3.3 Effect of particle size on peroxidase-like activity of biochar

The biochar peroxidase-like activity also depends on the particle size, as documented in Fig. 2b for maize cob (MC) biochar. As expected, smaller biochar particles exhibit higher activity. A similar situation was also observed in the case of nanomaterials mimicking peroxidases; this phenomenon may be due to the smaller particles having a greater surface-to-volume ratio to interact with their substrates. This observation suggests that selective fabrication of peroxidase-like materials with different size and shape is very important to modulate their catalytic activities (Jv et al. 2010; Peng et al. 2015).

3.4 Effect of reaction conditions on peroxidase-like activity of biochar

The influence of the reaction temperature on the oxidation of DPD catalyzed by the woody biochar BC1 was investigated in the range from 4 °C to 62 °C (Fig. 2c). The oxidation of DPD reached the maximum value at temperature ca 32 °C; relatively high activity (more than 77%, taking maximum activity value as 100%) can be observed between 4 °C and 42 °C. However, higher values of the reaction temperature led to the substantial decrease in the enzyme-like activity. Similar temperature optima were also observed for some other peroxidase-like materials, such as $CoFe_2O_4$ nanoparticles (Zhang et al. 2015), magnetic iron oxide nanoparticles (Gao et al. 2007), hemin bound to carbon nanotubes (Zhang et al. 2013), etc. Such behavior seems to be general for both real peroxidases and peroxidase-like materials.

The peroxidase-like activity of biochars also depends on the pH value of the reaction mixture. Figure 2d shows that the highest activity was observed at pH 4 for the woody biochar BC1. When compared with other natural catalysts (enzymes) or enzyme-like materials, the same or very similar pH value was also optimal for horseradish peroxidase (Jiao et al. 2012), V_2O_3-ordered mesoporous carbon composite (Han et al. 2015), $CoFe_2O_4$ nanoparticles (Zhang et al. 2015), ceria (CeO_2) nanoparticles (Jiao et al. 2012) or hemin bound to carbon nanotubes (Zhang et al. 2013). Also in this case we can say that similar behavior has been found very often, both for natural and synthetic peroxidases.

3.5 Effects of magnetic modification of biochar on its peroxidase-like activity

Based on the fact that the magnetic iron oxide particles also exhibit peroxidase-like activity, magnetically responsive biochar derivatives were prepared and tested (Safarik et al. 2016). As presented in Table 5, the binding of microwave-synthesized iron oxide magnetic particles on biochar surface led to the significant increases in peroxidase-like activities for selected biochar samples (BC1, IND and OL7). All magnetically modified biochars were prepared using the same procedure, thus leading to a similar amount of magnetic iron oxide particles bound on the biochar surface. That is why the differences in peroxidase-like activities between native and magnetically modified biochars were similar (ca. 0.24–0.28 absorbance unit).

Magnetic modification of biochar is important from two points, namely, the possibility of simple magnetic separation of magnetic biochar from various environments, and the addition of new peroxidase-like activity to the composite material. Enzyme kinetic constants K_m and V_{max} for both native biochar BC1 and its magnetic derivative MBC1 are given in Chapter 3.1 and Table 4. Similarly to two enzymes acting to one substrate (Dixon and Webb 1964), the V_{max} value for magnetic biochar was higher than V_{max} for native biochar.

3.6 Electrochemical measurements

Cyclic voltammetry measurement (CVM) was employed to investigate the peroxidase-like activity of biochar sample (see Fig. S3). A set of CVMs was recorded by sweeping the potential range from 0.0 to −1.0 V at a constant scan rate of 20 mV s^{-1} using a bare GC electrode or a GC electrode modified with a tested sample in the absence (dashed lines) or in the presence (area) of 4 mmol L^{-1} hydrogen peroxide. As can be seen in Fig. S3, the peak of H_2O_2 decomposition recorded at $E = -1.34$ V for an electrode modified with biochar is significantly higher compared to the response of

Table 5 Comparison of peroxidase-like activities of native and magnetically modified biochars

Sample	A_{551} (native)	A_{551} (magnetic)
BC1	0.639 ± 0.139	0.919 ± 0.089
IND	0.584 ± 0.067	0.826 ± 0.205
OL7	0.125 ± 0.005	0.407 ± 0.011

the unmodified electrode indicating the potential of biochar to serve as a successful catalyst for the decomposition of the target molecule (H_2O_2). As a single reduction peak is observed, one can conclude that the reaction mechanism obeys the reported $2e^-$, $2H^+$ reduction pathway according to the following equations (Cai et al. 2018):

$$H_2O_2 + H^+ + e^- \rightarrow OH^{\cdot}_{(ads)} + H_2O \quad (1)$$

$$OH^{\cdot}_{(ads)} + H^+ + e^- \rightarrow H_2O \quad (2)$$

A small shoulder located at $E = -0.43$ V supports this hypothesis. Hydrogen peroxide undergoes one proton and one electron exchange reaction to form an adsorbed hydroxyl radical and water as shown in Eq. (1). These products further undergo another one proton and one electron reaction [Eq. (2)] resulting in a two peaks response.

3.7 Potential technological application of biochar peroxidase-like activity

It is well known that enzyme based technologies have been successfully used for bioremediation of recalcitrant xenobiotic compounds from the natural environment. Different types of microbial and plant enzymes exhibiting bioremediation activities have been isolated and used. Enzyme immobilization and genetic engineering approaches led to enzyme preparations with improved half-life, stability and activity.

Horseradish peroxidase is known to be effective in the removal of a wide spectrum of aromatic compounds (phenols, biphenols, anilines) in the presence of hydrogen peroxide and in the degradation, decolorization and precipitation of important industrial dyes (Ulson de Souza et al. 2007). Other types of peroxidases from various sources can also be efficient for other important pollutants removal (e.g., endocrine disruptive chemicals, polychlorinated biphenyls, chlorinated alkanes and alkenes, phenoxy alkanoic and triazine herbicides, chlorinated dioxins and chlorinated insecticides) (Bansal and Kanwar 2013).

Peroxidase catalyzed degradation of various dyes has been studied, namely, Remazol Turquoise Blue G and Lanaset Blue 2R (Ulson de Souza et al. 2007), Remazol blue and crystal violet (Bhunia et al. 2001) or bromophenol blue and methyl orange (Liu et al. 2006). Inactivation of the enzyme in the presence of the dye was found to be the major limitation in potential commercial application of the technique for effluent treatment in the dye manufacturing industry (Bhunia et al. 2001).

However, recently discovered nanozymes of different types and their peroxidase mimetics could solve this problem. They may offer the potential bioremediation ability towards a broad range of toxic, carcinogenic and hazardous environmental pollutants at low cost (Sharma et al. 2018). Biochar accompanies other carbon materials (e.g., carbon nanotubes, graphene derivatives, fullerenes, carbon nanohorns or carbon nanodots), where peroxidase-like activity has been detected recently and used, e.g., for methyl red, methyl orange, rhodamine B, methylene blue, orange II or phenolic compound degradation (Sun et al. 2018). Importantly, biochar can be prepared by simpler processes and in larger quantities in comparison with these special carbon structures.

In our study, we tested the decolorization of model water soluble organic dye crystal violet containing a triphenylmethane structure, using two peroxidase mimetics, namely, biochar (BC1) and microwave-synthesized iron oxide particles. Both materials react well with typical peroxidase substrates in the presence of hydrogen peroxide (see Fig. 3, left), but only biochar was able to decolorize crystal violet in the presence of H_2O_2 (see Fig. 3, right). The decolorization was caused almost exclusively by the biochar catalytic activity because no visible decolorization was caused by hydrogen peroxide itself and no relevant adsorption of dye to biochar was observed under the selected reaction conditions (Fig. 3, middle).

As was mentioned for the reaction with the DPD substrate, we have also tested the possible quenching of radicals by ascorbic acid during decolorization reactions.

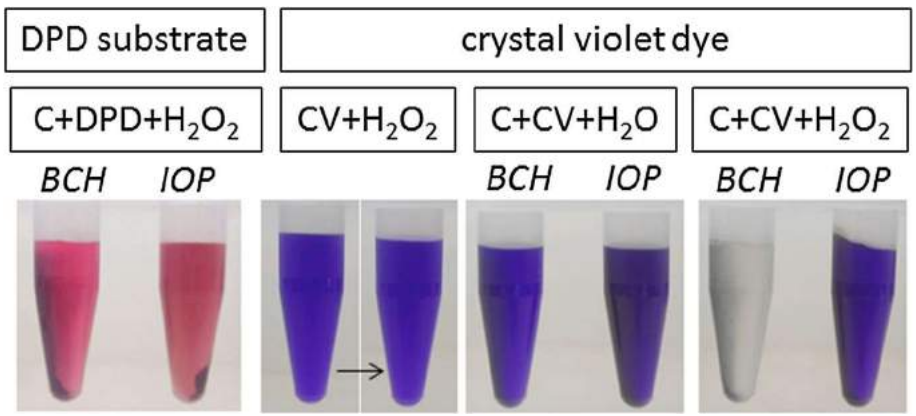

Fig. 3 Comparison of biochar and iron oxide particles catalytic properties used for the reaction with DPD substrate and the decolorization of crystal violet dye solution. *BCH* biochar BC1, *IOP* magnetic iron oxide particles prepared by microwave-assisted synthesis, *C* catalyst (*BCH* or *IOP*), *DPD N,N*-diethyl-*p*-phenylenediamine, *CV* crystal violet (color online)

Catalytic activity of biochars was affected (inhibited) by the presence of AA. This was demonstrated by the decolorization of a crystal violet solution by the BC1 sample. In this case, the generation of radicals also plays an important role in the catalytic mechanism.

Biochar exhibited catalytic and decolorization activity not only in distilled water, but also in fish pond water containing suspended solids and dissolved organic matter. Three typical pond water samples were analyzed with the same results. As can be seen in Fig. 4, presenting the results using Zdrahanka pond water, there was no color change after single addition of hydrogen peroxide or biochar only to crystal violet solutions (Fig. 4a–c). However, the addition of both biochar and hydrogen peroxide to crystal violet dissolved in fish pond water led to total dye decolorization in 10 min (Fig. 4d).

Our experiments clearly show the potential of biochar in technological applications. In addition, differences in the specificity of enzyme mimetics can be clearly seen in these examples. The decolorization of organic dyes by biochar-based materials in the presence of hydrogen peroxide will be investigated systematically in a future study.

4 Conclusions

Biochar production represents a typical example of a circular bio-economy process. Various types of biochar were prepared by pyrolysis of diverse biomass feedstocks. For the first time, peroxidase-like activity of biochar-based materials was detected. All tested samples of biochar exhibited peroxidase-like activity. Biochars oxidized specific organic substrates (DPD or TMB) in the presence of hydrogen peroxide and could be used repeatedly at least ten times without any loss of catalytic activity. Magnetic modification with iron oxides increased the catalytic activity of biochar-based composites. In general, differences in the peroxidase-like activities between biochar samples are affected by the type of feedstock, pyrolysis temperature and various modification treatments. Biochar exhibited catalytic and decolorization activities of crystal violet not only in distilled water, but also in fish pond water containing suspended solids and dissolved organic matter.

Based on these findings, it can be concluded that biochar is a promising alternative material to common peroxidases for industrial purposes. This material exhibits many advantages; especially, it can be prepared from widely available biomass waste materials by relatively simple procedures reducing the costs of resulting materials. Availability of large quantities of biochar and its better resistance to external conditions compared to enzyme biomolecules can also be very important and useful for industrial applications. The existing peroxidase-like activity can have interesting applications in environmental technologies as a part of oxidative processes or as peroxidase enzyme replacement.

Smart biochar-based materials exhibiting enzyme-like activities can be considered as the third biochar generation, following the second generation biochars which are applied as efficient adsorbents of a broad range of organic or inorganic compounds and the first generation biochars that are utilized as soil amendment in agriculture.

Acknowledgements This research was supported by the Ministry of the Interior of the Czech Republic (Project No. VI20162019017) and by the ERDF projects “New Composite Materials for Environmental

Fig. 4 Decolorization of crystal violet dissolved in distilled water, untreated fish pond water and filtered fish pond water (from left to right) by catalytic activity of biochar BC1. **a** Water solutions of crystal violet; **b** water solutions of crystal violet with the addition of hydrogen peroxide; **c** water solutions of crystal violet with the addition of biochar; **d** water solutions of crystal violet with the addition of biochar and hydrogen peroxide. Incubation time was 10 min (color online)

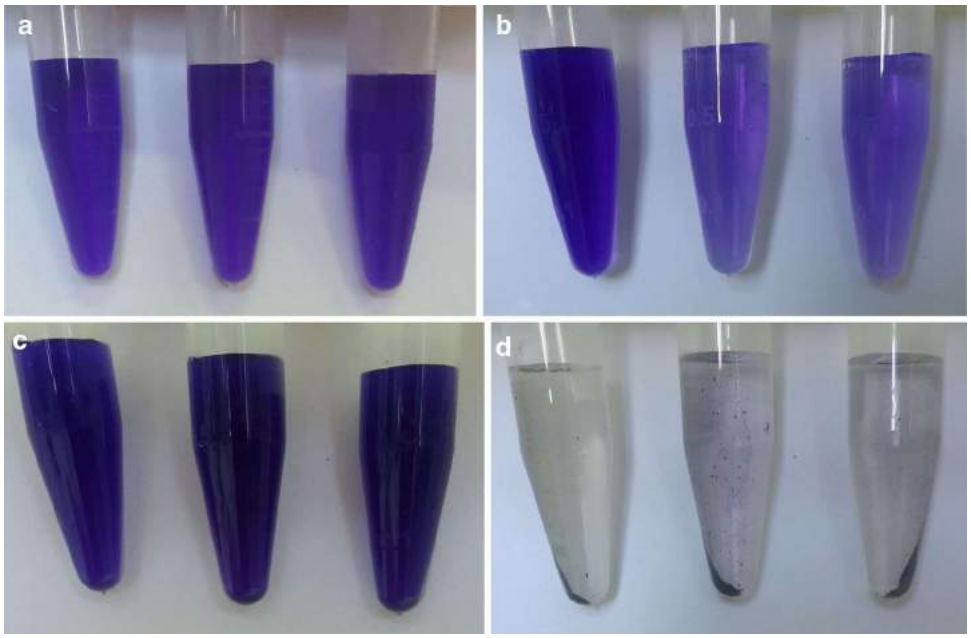

Applications" (No. CZ.02.1.01/0.0/0.0/17_048/0007399) and "Development of pre-applied research in nanotechnology and biotechnology" (No. CZ.02.1.01/0.0/0.0/17_048/0007323).

Compliance with ethical standards

Conflict of interest There are no conflicts to declare.

References

Asada T, Oikawa K, Kawata K, Ishihara S, Iyobe T, Yamada A (2004) Study of removal effect of bisphenol A and beta-estradiol by porous carbon. J Health Sci 50(6):588–593

Astruc D, Lu F, Aranzaes JR (2005) Nanoparticles as recyclable catalysts: the frontier between homogeneous and heterogeneous catalysis. Angew Chem-Int Ed 44:7852–7872

Bachmann HJ, Bucheli TD, Dieguez-Alonso A, Fabbri D, Knicker H, Schmidt HP, Ulbricht A, Becker R, Buscaroli A, Buerge D, Cross A, Dickinson D, Enders A, Esteves VI, Evangelou MWH, Fellet G, Friedrich K, Guerrero GG, Glaser B, Hanke UM, Hanley K, Hilber I, Kalderis D, Leifeld J, Masek O, Mumme J, Carmona MP, Pereira RC, Rees F, Rombola AG, de la Rosa JM, Sakrabani R, Sohi S, Soja G, Valagussa M, Verheijen F, Zehetner F (2016) Toward the standardization of biochar analysis: the COST Action TD1107 interlaboratory comparison. J Agric Food Chem 64(2):513–527

Bader H, Sturzenegger V, Hoigne J (1988) Photometric method for the determination of low concentrations of hydrogen peroxide by the peroxidase catalyzed oxidation of *N*,*N*-diethyl-*p*-phenylenediamine (DPD). Water Res 22(9):1109–1115

Bansal N, Kanwar SS (2013) Peroxidase(s) in environment protection. Sci World J 2013:9 **(Article ID 714639)**

Bhunia A, Durani S, Wangikar PP (2001) Horseradish peroxidase catalyzed degradation of industrially important dyes. Biotechnol Bioeng 72(5):562–567

Bilal M, Asgher M, Parra-Saldivar R, Hu H, Wang W, Zhang X, Iqbal HMN (2017) Immobilized ligninolytic enzymes: an innovative and environmental responsive technology to tackle dye-based industrial pollutants—a review. Sci Total Environ 576:646–659

Cai X, Tanner EEL, Lin C, Ngamchuea K, Foord JS, Compton RG (2018) The mechanism of electrochemical reduction of hydrogen peroxide on silver nanoparticles. Phys Chem Chem Phys 20:1608–1614

Chang Q, Deng K, Zhu L, Jiang G, Yu C, Tang H (2009) Determination of hydrogen peroxide with the aid of peroxidase-like Fe_3O_4 magnetic nanoparticles as the catalyst. Microchim Acta 165(3):299

Chen W, Chen J, Feng Y-B, Hong L, Chen Q-Y, Wu L-F, Lin X-H, Xia X-H (2012) Peroxidase-like activity of water-soluble cupric oxide nanoparticles and its analytical application for detection of hydrogen peroxide and glucose. Analyst 137(7):1706–1712

Chen X, Zhai N, Snyder JH, Chen QS, Liu PP, Jin LF, Zheng QX, Lin FC, Hu JM, Zhou HN (2015) Colorimetric detection of Hg^{2+} and Pb^{2+} based on peroxidase-like activity of graphene oxide-gold nanohybrids. Anal Methods 7(5):1951–1957

Chuah LF, Klemeš JJ, Yusup S, Bokhari A, Akbar MM (2017) A review of cleaner intensification technologies in biodiesel production. J Clean Product 146:181–193

Cui R, Han Z, Zhu J-J (2011) Helical carbon nanotubes: intrinsic peroxidase catalytic activity and its application for biocatalysis and biosensing. Chem Eur J 17(34):9377–9384

Deng HH, Hong GL, Lin FL, Liu AL, Xia XH, Chen W (2016) Colorimetric detection of urea, urease, and urease inhibitor based on the peroxidase-like activity of gold nanoparticles. Anal Chim Acta 915:74–80

Ding CP, Yan YH, Xiang DS, Zhang CL, Xian YZ (2016) Magnetic Fe_3S_4 nanoparticles with peroxidase-like activity, and their use in a photometric enzymatic glucose assay. Microchim Acta 183(2):625–631

Dixon M, Webb EC (1964) Enzymes, 2nd edn. Academic Press, New York

Dong W, Zhuang Y, Li S, Zhang X, Chai H, Huang Y (2018) High peroxidase-like activity of metallic cobalt nanoparticles encapsulated in metal–organic frameworks derived carbon for biosensing. Sens Actuator B Chem 255:2050–2057

EBC (2019) EBC European biochar certificate—Guidelines for a sustainable production of biochar. Version 8.3E of 1st September 2019. http://www.european-biochar.org/en/download

El-Naggar A, El-Naggar AH, Shaheen SM, Sarkar B, Chang SX, Tsang DCW, Rinklebe J, Ok YS (2019a) Biochar composition-dependent impacts on soil nutrient release, carbon mineralization, and potential environmental risk: a review. J Environ Manag 241:458–467

El-Naggar A, Lee SS, Rinklebe J, Farooq M, Song H, Sarmah AK, Zimmerman AR, Ahmad M, Shaheen SM, Ok YS (2019b) Biochar application to low fertility soils: a review of current status, and future prospects. Geoderma 337:536–554

Fang GD, Gao J, Liu C, Dionysiou DD, Wang Y, Zhou DM (2014) Key role of persistent free radicals in hydrogen peroxide activation by biochar: implications to organic contaminant degradation. Environ Sci Technol 48(3):1902–1910

Gao LZ, Zhuang J, Nie L, Zhang JB, Zhang Y, Gu N, Wang TH, Feng J, Yang DL, Perrett S, Yan X (2007) Intrinsic peroxidase-like activity of ferromagnetic nanoparticles. Nature Nanotechnol 2(9):577–583

Gao LZ, Giglio KM, Nelson JL, Sondermann H, Travis AJ (2014) Ferromagnetic nanoparticles with peroxidase-like activity enhance the cleavage of biological macromolecules for biofilm elimination. Nanoscale 6(5):2588–2593

Garg B, Bisht T, Ling YC (2015) Graphene-based nanomaterials as efficient peroxidase mimetic catalysts for biosensing applications: an overview. Molecules 20(8):14155–14190

Golchin J, Golchin K, Alidadian N, Ghaderi S, Eslamkhah S, Eslamkhah M, Akbarzadeh A (2017) Nanozyme applications in biology and medicine: an overview. Artif Cells Nanomed Biotechnol 45(6):1–8

Guo YL, Liu XY, Yang CD, Wang XD, Wang D, Iqbal A, Liu WS, Qin WW (2015) Synthesis and peroxidase-like activity of cobalt@carbon-dots hybrid material. ChemCatChem 7(16):2467–2474

Haider W, Hayat A, Raza Y, Chaudhry AA, Ihtesham Ur R, Marty JL (2015) Gold nanoparticle decorated single walled carbon nanotube nanocomposite with synergistic peroxidase like activity for D-alanine detection. RSC Adv 5(32):24853–24858

Han L, Zeng LX, Wei MD, Li CM, Liu AH (2015) A V_2O_3-ordered mesoporous carbon composite with novel peroxidase-like activity towards the glucose colorimetric assay. Nanoscale 7(27):11678–11685

Hayat A, Haider W, Raza Y, Marty JL (2015) Colorimetric cholesterol sensor based on peroxidase like activity of zinc oxide nanoparticles incorporated carbon nanotubes. Talanta 143:157–161

Huang M, Gu JL, Elangovan SP, Li YS, Zhao WR, Iijima T, Yamazaki Y, Shi JL (2013) Intrinsic peroxidase-like catalytic activity of hydrophilic mesoporous carbons. Chem Lett 42(8):785–787

Huang Y, Ren J, Qu X (2019) Nanozymes: classification, catalytic mechanisms, activity regulation, and applications. Chem Rev 119(6):4357–4412

Jiang T, Song Y, Wei TX, Li H, Du D, Zhu MJ, Lin YH (2016) Sensitive detection of *Escherichia coli* O157:H7 using Pt–Au bimetal nanoparticles with peroxidase-like amplification. Biosens Bioelectron 77:687–694

Jiao X, Song HJ, Zhao HH, Bai W, Zhang LC, Lv Y (2012) Well-redispersed ceria nanoparticles: promising peroxidase mimetics for H_2O_2 and glucose detection. Anal Methods 4(10):3261–3267

Jv Y, Li BX, Cao R (2010) Positively-charged gold nanoparticles as peroxidase mimic and their application in hydrogen peroxide and glucose detection. Chem Commun 46(42):8017–8019

Lee J, Kim K-H, Kwon EE (2017) Biochar as a catalyst. Renew Sust Energ Rev 77:70–79

Li RM, Zhen MM, Guan MR, Chen DQ, Zhang GQ, Ge JC, Gong P, Wang CR, Shu CY (2013a) A novel glucose colorimetric sensor based on intrinsic peroxidase-like activity of C-60-carboxyfullerenes. Biosens Bioelectron 47:502–507

Li X, Shen Q, Zhang D, Mei X, Ran W, Xu Y, Yu G (2013b) Functional groups determine biochar properties (pH and EC) as studied by two-dimensional ^{13}C NMR correlation spectroscopy. PLoS One 8(6):e65949

Li R, Huang H, Wang JJ, Liang W, Gao P, Zhang Z, Xiao R, Zhou B, Zhang X (2019) Conversion of Cu(II)-polluted biomass into an environmentally benign Cu nanoparticles-embedded biochar composite and its potential use on cyanobacteria inhibition. J Clean Prod 216:25–32

Liu J-Z, Wang T-L, Ji L-N (2006) Enhanced dye decolorization efficiency by citraconic anhydride-modified horseradish peroxidase. J Mol Catal B Enzym 41(3–4):81–86

Melnikova L, Pospiskova K, Mitroova Z, Kopcansky P, Safarik I (2014) Peroxidase-like activity of magnetoferritin. Microchim Acta 181(3–4):295–301

Mu JS, Li J, Zhao X, Yang EC, Zhao XJ (2016) Cobalt-doped graphitic carbon nitride with enhanced peroxidase-like activity for wastewater treatment. RSC Adv 6(42):35568–35576

Oliveira FR, Patel AK, Jaisi DP, Adhikari S, Lu H, Khanal SK (2017) Environmental application of biochar: current status and perspectives. Bioresour Technol 246:110–122

Park JY, Jeong HY, Kim MI, Park TJ (2015) Colorimetric detection system for *Salmonella typhimurium* based on peroxidase-like activity of magnetic nanoparticles with DNA aptamers. J Nanomater 2015:2 **(Article ID 527126)**

Peng FF, Zhang Y, Gu N (2008) Size-dependent peroxidase-like catalytic activity of Fe_3O_4 nanoparticles. Chin Chem Lett 19(6):730–733

Peng YH, Wang ZY, Liu WS, Zhang HL, Zuo W, Tang HA, Chen FJ, Wang BD (2015) Size- and shape-dependent peroxidase-like catalytic activity of $MnFe_2O_4$ nanoparticles and their applications in highly efficient colorimetric detection of target cancer cells. Dalton Trans 44(28):12871–12877

Qambrani NA, Rahman MM, Won S, Shim S, Ra C (2017) Biochar properties and eco-friendly applications for climate change mitigation, waste management, and wastewater treatment: a review. Renew Sust Energ Rev 79:255–273

Qiao FM, Chen LJ, Li XN, Li LF, Ai SY (2014) Peroxidase-like activity of manganese selenide nanoparticles and its analytical application for visual detection of hydrogen peroxide and glucose. Sens Actuator B Chem 193:255–262

Safarik I, Safarikova M (2014) One-step magnetic modification of non-magnetic solid materials. Int J Mater Res 105(1):104–107

Safarik I, Maderova Z, Pospiskova K, Schmidt HP, Baldikova E, Filip J, Krizek M, Malina O, Safarikova M (2016) Magnetically modified biochar for organic xenobiotics removal. Water Sci Technol 74(7):1706–1715

Safavi A, Sedaghati F, Shahbaazi H, Farjami E (2012) Facile approach to the synthesis of carbon nanodots and their peroxidase mimetic function in azo dyes degradation. RSC Adv 2(19):7367–7370

Sewu DD, Boakye P, Woo SH (2017) Highly efficient adsorption of cationic dye by biochar produced with Korean cabbage waste. Bioresour Technol 224:206–213

Sharma B, Dangi AK, Shukla P (2018) Contemporary enzyme based technologies for bioremediation: a review. J Environ Manag 210:10–22

Singh B, Fang Y, Cowie BCC, Thomsen L (2014) NEXAFS and XPS characterisation of carbon functional groups of fresh and aged biochars. Org Geochem 77:1–10

Song Y, Qu K, Zhao C, Ren J, Qu X (2010) Graphene oxide: intrinsic peroxidase catalytic activity and its application to glucose detection. Adv Mater 22(19):2206–2210

Sun HY, Jiao XL, Han YY, Jiang Z, Chen DR (2013) Synthesis of Fe_3O_4–Au nanocomposites with enhanced peroxidase-like activity. Eur J Inorg Chem 1:109–114

Sun HJ, Zhao AD, Gao N, Li K, Ren JS, Qu XG (2015) Deciphering a nanocarbon-based artificial peroxidase: chemical identification of the catalytically active and substrate-binding sites on graphene quantum dots. Angew Chem Int Edit 54(24):7176–7180

Sun H, Zhou Y, Ren J, Qu X (2018) Carbon nanozymes: enzymatic properties, catalytic mechanism, and applications. Angew Chem Int Edit 57(30):9224–9237

Tian ZM, Li J, Zhang ZY, Gao W, Zhou XM, Qu YQ (2015) Highly sensitive and robust peroxidase-like activity of porous nanorods of ceria and their application for breast cancer detection. Biomaterials 59:116–124

Trazzi PA, Leahy JJ, Hayes MHB, Kwapinski W (2016) Adsorption and desorption of phosphate on biochars. J Environ Chem Eng 4(1):37–46

Ulson de Souza SMAG, Forgiarini E, Ulson de Souza AA (2007) Toxicity of textile dyes and their degradation by the enzyme horseradish peroxidase (HRP). J Hazard Mater 147(3):1073–1078

Varma RS (2016) Greener and sustainable trends in synthesis of organics and nanomaterials. ACS Sustain Chem Eng 4:5866–5878

Wan D, Li WB, Wang GH, Wei XB (2016) Shape-controllable synthesis of peroxidase-like Fe_3O_4 nanoparticles for catalytic removal of organic pollutants. J Mater Eng Perform 25(10):4333–4340

Wang S, Chen W, Liu AL, Hong L, Deng HH, Lin XH (2012a) Comparison of the peroxidase-like activity of unmodified, amino-modified, and citrate-capped gold nanoparticles. ChemPhysChem 13(5):1199–1204

Wang W, Jiang XP, Chen KZ (2012b) Iron phosphate microflowers as peroxidase mimic and superoxide dismutase mimic for biocatalysis and biosensing. Chem Commun 48(58):7289–7291

Wang RZ, Huang DL, Liu YG, Zhang C, Lai C, Wang X, Zeng GM, Gong XM, Duan A, Zhang Q, Xu P (2019) Recent advances in biochar-based catalysts: properties, applications and mechanisms for pollution remediation. Chem Eng J 371:380–403

Wei H, Wang EK (2013) Nanomaterials with enzyme-like characteristics (nanozymes): next-generation artificial enzymes. Chem Soc Rev 42(14):6060–6093

Wu XC, Zhang Y, Han T, Wu HX, Guo SW, Zhang JY (2014) Composite of graphene quantum dots and Fe_3O_4 nanoparticles: peroxidase activity and application in phenolic compound removal. RSC Adv 4(7):3299–3305

Wu J, Wang X, Wang Q, Lou Z, Li S, Zhu Y, Qin L, Wei H (2019) Nanomaterials with enzyme-like characteristics (nanozymes): next-generation artificial enzymes (II). Chem Soc Rev 48:1004–1076

Xie JX, Cao HY, Jiang H, Chen YJ, Shi WB, Zheng HZ, Huang YM (2013) Co_3O_4-reduced graphene oxide nanocomposite as an effective peroxidase mimetic and its application in visual biosensing of glucose. Anal Chim Acta 796:92–100

Yu YZ, Ju P, Zhang D, Han XX, Yin XF, Zheng L, Sun CJ (2016) Peroxidase-like activity of $FeVO_4$ nanobelts and its analytical application for optical detection of hydrogen peroxide. Sens Actuator B Chem 233:162–172

Zhang Y, Xu C, Li B (2013) Self-assembly of hemin on carbon nanotube as highly active peroxidase mimetic and its application for biosensing. RSC Adv 3(17):6044–6050

Zhang K, Zuo W, Wang ZY, Liu J, Li TR, Wang BD, Yang ZY (2015) A simple route to $CoFe_2O_4$ nanoparticles with shape and size control and their tunable peroxidase-like activity. RSC Adv 5(14):10632–10640

Zheng AX, Zhang XL, Gao J, Liu XL, Liu JF (2016) Peroxidase-like catalytic activity of copper ions and its application for highly sensitive detection of glypican-3. Anal Chim Acta 941:87–93

Zhu WF, Zhang J, Jiang ZC, Wang WW, Liu XH (2014) High-quality carbon dots: synthesis, peroxidase-like activity and their application in the detection of H_2O_2, Ag^+ and Fe^{3+}. RSC Adv 4(33):17387–17392